A consideration of the accuracy and application of the Brather approximation for the transformation of dielectric relaxation data from the time domain to the frequency domain

George P. Simon
Department of Materials Engineering, Monash University, Clayton, Victoria 3168, Australia

and Graham Williams*
Department of Chemistry, University College of Swansea, Swansea SA2 8PP, UK
(Received 15 May 1992)

The methodology for conversion of transient current data in the time domain into dielectric loss data in the frequency domain using the Brather approximation is described. A test of the accuracy of the approximation is made using the 'stretched exponential' relaxation function (Kohlrausch–Williams–Watts function) for which the Fourier transform has been previously tabulated for a range of exponent $\beta(0 < \beta \leqslant 1)$. As an example of the application of the Brather approximation we report ultra-low frequency dielectric loss data ($10^{-3.5}$ to $10^{-0.4}$) for a liquid-crystalline side-chain polymer as derived from transient current data.

(Keywords: dielectric; polymer; relaxation; Fourier; liquid crystalline)

INTRODUCTION

Ultra-low frequency dielectric measurements of solid polymers are conveniently performed by measuring the transient current $I(t)$ obtained following the step removal of a steady voltage V from a sample, and performing a Fourier transform of $(I(t)/V)$ to yield the components of the complex dielectric permittivity via the relation[1]:

$$\varepsilon(\omega) - \varepsilon_\infty = \int_0^\infty \varphi(t) \exp(-i\omega t)\, dt \qquad (1)$$

where $\varphi(t) = I(t)/VC_0$ and C_0 is the geometric capacitance of the sample, $\omega = 2\pi f$ where f is the frequency of measurement (Hz) and ε_∞ is the limiting high frequency dielectric permittivity. The transient current method has been used to obtain low frequency dielectric relaxation data for polymer solids for many years[1] and has been improved by Mopsik[2,3] using modern computational methods and modern instrumentation, allowing data to be obtained in the range 10^{-4} to 10^4 Hz. Mopsik[2,3] showed that loss factors ranging from several units to very small values ($\sim 10^{-5}$) could be measured for solid polymer materials.

During the course of our studies of the dielectric properties of thermotropic liquid-crystalline side-chain polymers[4–6] it became apparent that a convenient method for the transformation of transient current data into dielectric loss data was that due to Brather[7] which is a generalization of the point-by-point transformation method originally developed by Hamon[8]. The Brather approximation was used by Ribelles and Calleja[9] to obtain ultra-low frequency dielectric loss data for solid poly(n-butyl methacrylate) and subsequently we applied the approximation to transient current data for homeotropically aligned and unaligned samples of a siloxane liquid-crystalline polymer in its smectic phase[6].

Some time ago it was found that a satisfactory fit of the dielectric dispersion and absorption curves for the primary (α) relaxation in amorphous polymers[10–13] and low molar mass glass-forming liquids[14] could be obtained using a 'stretched exponential function', $\Phi(t)$, of the following form:

$$\Phi(t) = \exp - (t/\tau_0)^{\beta} \qquad (2)$$

where $0 < \beta \leqslant 1$, τ_0 is an effective relaxation time and $\varphi(t)$ in equation (1) is related to $\Phi(t)$ by the relation $\varphi(t) = |d\Phi(t)/dt|$. This is known as the Kohlrausch–Williams–Watts (KWW) function. The normalized permittivity and loss are calculated using the integral transforms:

$$\frac{\varepsilon'(\omega) - \varepsilon_\infty}{\varepsilon_0 - \varepsilon_\infty} = -\int_0^\infty \dot{\Phi}(t) \cos \omega t\, dt \qquad (3)$$

$$\frac{\varepsilon''(\omega)}{\varepsilon_0 - \varepsilon_\infty} = -\int_0^\infty \dot{\Phi}(t) \sin \omega t\, dt \qquad (4)$$

In the earlier work, the accuracy of the point-by-point transformation method $(I(t), t) \rightarrow (\varepsilon''(\omega), \omega)$, where $\omega = 0.2\pi/t$, of Hamon[8] for the KWW function was investigated and it was shown that poor accuracy was obtained for $\log \omega\tau_0 < 1$. Subsequently Koizumi and

*To whom correspondence should be addressed

0032-3861/93/102038-07

Kita[15] gave tables of the normalized permittivity and loss as a function of $\log \omega\tau_0$ for $0.3 \leqslant \beta \leqslant 1.0$ and $-3.0 < \log \omega\tau < 3.0$ as derived numerically from equations (2)–(4).

In the present work we outline the methodology for using the Brather approximation and we assess its accuracy for the particular case of the KWW function (equation (2)). The Brather approximation involves the use of a set of $I(t)$ values to obtain $\varepsilon''(\omega)$ data at each chosen value of ω. A part of this process is to extrapolate the derived $\varepsilon''(\omega)$ data to values of ω larger than those calculated initially. This process is iterated and leads to a convergence of the calculated $\varepsilon''(\omega)$ values in the low-frequency band. Thus the method provides a means of reducing errors associated with the truncation of the Fourier transform due to band-limited data[2,3]. We then proceed to show how the method may be applied to experimental transient-current data for a liquid-crystalline polymer.

THEORETICAL BACKGROUND

The Hamon transformation method[8] assumes that:

$$\varphi(t) = ct^{-n} \tag{5}$$

where c and n are material constants. It was shown by Hamon[8] for $0 < n < 2$ that:

$$\varepsilon''(\omega) = \frac{\varphi(t)}{\omega} \tag{6a}$$

$$\omega = 0.2\pi/t \tag{6b}$$

This point-by-point transformation is accurate for frequencies above the loss-factor maximum, but is inaccurate for frequencies below that loss peak, as has been demonstrated by Williams and coworkers for the particular cases of the Cole–Cole relaxation function[16] and the KWW function[11,12]. However, the function (equation (5)) can only be true over a limited segment of $\varphi(t)$. Another method for obtaining $\varepsilon''(\omega)$ from transient data is to carry out the Fourier transform directly. However, experimental data for $\varphi(t)$ are always band-limited, leading to truncation errors through lack of data at both short and long times. Such errors affect the calculated $\varepsilon''(\omega)$ values at all values of ω. Experimentally, the problem of rapid data acquisition is of importance because the currents at short times make an important contribution to the Fourier integral. Mopsik[2,3] extrapolated his short-time data towards the time-origin using a cubic-spline method. While this proved satisfactory, large amounts of computing power were required, which would not normally be available using a personal computer. Also, a degree of artificiality is introduced by using a curve-fitting procedure to produce more data points.

Brather[7] derived equations which allow $\varepsilon''(\omega)$ for a chosen value of ω to be determined from a sequence of $I(t)$ values. The method is far more accurate than the Hamon methods, as we shall demonstrate. In its operation, the transient data themselves are sufficient if the times for measurement of $I(t)$ are small compared with ω^{-1}. However, to span an entire loss curve a knowledge of $\varepsilon''(\omega)$ at values of ω higher than those calculated is required, so it is necessary either (i) to extrapolate the initially calculated $\varepsilon''(\omega)$ data to higher frequencies, or (ii) to complement the transient data with experimental low frequency measurements (10^{-1} to 10^2 Hz), e.g. using a Scheiber bridge[17]. These additional values of $\varepsilon''(\omega)$ are inserted into the Brather equations and are necessary in order to reduce truncation errors, as we have indicated in the Introduction.

Brather[7] deduced the following equations for the loss factor, which give values that would have an error of $\leqslant 3\%$.

$$\varepsilon''(\omega) = \frac{1}{\omega\varepsilon_0}\left[\sum_{j=-3}^{l-1} a_j^{(l)}\varphi(1/2^j\omega) + \sum_{j=1}^{l+2} b_j^{(l)}\varepsilon''(2^j\omega)\right] \pm \text{error term } (\varepsilon''(\omega), \omega) \tag{7}$$

for $l = 1$–3

where $a_j^{(l)}$ and $b_j^{(l)}$ are given in Table 1 of reference 7.

$$\varepsilon''(\omega) = \frac{1}{\omega\varepsilon_0}\Bigg[0.240\varphi(8/\omega) - 1.167\varphi(4/\omega) + 1.083\varphi(2/\omega) + \left(\frac{1.388}{4^l} + 0.61073\right)\varphi(1/\omega) + 0.6998\sum_{j=1}^{l-3}\frac{1}{4^j}\varphi(1/2^j\omega) + \frac{1}{4^l}\{8.4752\varphi(1/2^{l-2}\omega) + 5.12\varphi(1/2^{l-1}\omega)\}\Bigg] + \frac{1}{2^l}[-0.5407\varepsilon''(2^l\omega) + 1.1185\varepsilon''(2^{l+1}\omega) - 0.2074\varepsilon''(2^{l+2}\omega)] \pm \text{error term } (\varepsilon''(\omega), \omega) \tag{8}$$

for $l = 4$–7

If t_0 is the first value of time chosen from the $(\varphi(t), t)$ data, then for each value of l ($l = 1$–7), use of the data with the chosen values $(t_0 l)$ gives a value of $\varepsilon''(\omega)$ at ω, where

$$\omega = (2^{1-l})/t_0 \tag{9}$$

Thus each chosen value of t_0 gives loss factor values at seven frequencies. Increasing t_0 yields sets of loss factor values for lower frequencies (see equation (9)). The highest attainable frequency is obtained when $t_0 = t_{00}$, where t_{00} is the first time of measurement of $\varphi(t)$ and $l = 1$, so ω is equal to $\omega_{00} = 1/t_{00}$. As t_{00} is decreased, ω_{00} increases accordingly. The lowest attainable frequency occurs for $l = 7$ so that $\omega = 2^{-6}/t_0$. As t_0 is increased, so ω (measured) decreases accordingly. As indicated above, the Brather approximation relies on the replacement of $(\varphi(t), t)$ data in the range $0 < t < t_{00}$ by a set of values of $\varepsilon''(\omega)$ at frequencies higher than ω_{00} and are:

$$\varepsilon''(2^j\omega), \quad j = l, l+2 \text{ for } l = 1\text{–}3$$

$$\varepsilon''(2^l\omega), \quad \text{for } l = 4\text{–}7$$

Once these values are estimated by extrapolation of the loss curve for $\omega < \omega_{00}$ calculated in the first cycle of the Brather method, they may be re-inserted and this iteration performed until the loss values in the frequency range of Brather approximation coverage. Since the practical range of our experiments, conducted with a higher impedance ammeter, is between $10^{-0.5}$ and $10^{-3.5}$ Hz, a mid-frequency technique such as the Scheiber bridge[17] may provide experimental values of

loss factor in the range 10^{-1} to 10^{-2} Hz for use with the Brather equations. The approach we describe in the present paper, however, was to use the Hamon approximation on the same $(\varphi(t), t)$ data which we were also going to transform with the Brather equations to produce a 'first-guess' loss spectrum from which we extrapolate the required high frequency loss data for insertion into the Brather equations. The iteration was made using the Brather equations and inserting the improved high frequency data on each cycle until convergence of loss values in the Brather range was achieved. Such a procedure removes the need to do additional high frequency loss measurements using the Scheiber bridge or a similar technique.

METHODOLOGY OF THE BRATHER TECHNIQUE AND COMPUTER PROGRAM

The above process was translated to a programmable personal computer. The program was interactive, requiring manual intervention to extrapolate the loss curve to frequencies acquired for the input guess value of the dielectric loss. A schematic of the program is given below.

Step 1. Acquire $(\varphi(t), t)$ data by charging the sample at a voltage, V, and measuring the decay current following the step removal of the voltage.
Step 2. Carry out the Hamon approximation for conversion of $(\varphi(t), (t)) \rightarrow (\varepsilon''(\omega), \omega)$ (equations (6)).
Step 3. Select t_{00}, this being the first point at which you have good data.
Step 4. The given value of t_{00} and $l = 1$–7 will define the first-guess values of $\varepsilon''(\omega)$ required for the first cycle of the use of the Brather equations. Thereafter, manual extrapolations of $\varepsilon''(\omega)$ from calculated Brather values are used.
Step 5. Produce plot of $\varepsilon''(\omega)$ against $\log f$. If this is the first cycle or the values of $\varepsilon''(\omega)$ have not converged sufficiently, it is necessary to extrapolate to 'high' frequencies to obtain 'better-guess' values for input into step 4, and continue for $l = 1$–7 for the same t_{00}. Otherwise continue to next step.
Step 6. Choose a new t_0 ($t_0 > t_{00}$) and go back to step 4.

One exits from the cycle at the end of step 5 *either* because there are sufficient values of $(\varepsilon''(\omega), \omega)$ to define an acceptable spectrum *or* because the highest acceptable value of t_0, experimentally, has been exceeded. If one tries to use t_0 values that are too large, there will not be data at sufficiently long times to apply the Brather equations.

ACCURACY OF THE BRATHER APPROXIMATION AS APPLIED TO THE KWW FUNCTION

We have tested the accuracy of the Brather approximation as applied to the KWW function (equation (2)) by comparing results obtained using equations (7) and (8) with the numerical results for the KWW function given by Koizumi and Kita[15].

Since $\varphi(t) = |\mathrm{d}\Phi(t)/\mathrm{d}t|$ it follows from equation (2) that:

$$\varphi(t) = \frac{\bar{\beta}}{\tau_0}\left(\frac{t}{\tau_0}\right)^{\bar{\beta}-1} \exp -(t/\tau_0)^{\bar{\beta}} \qquad (10)$$

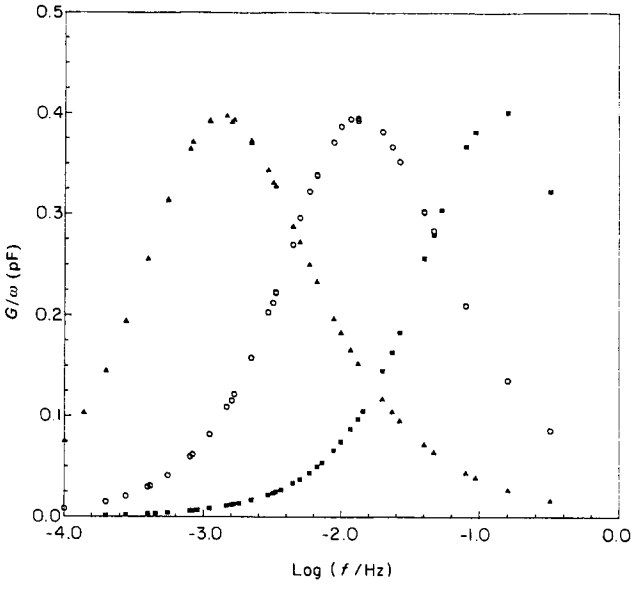

Figure 1 Normalized loss factor G/ω *versus* $\log f$ obtained using the Brather approximation applied to the KWW function (equation (2)); $\bar{\beta} = 0.75$. ▲, $\tau_0 = 100$; ○, $\tau_0 = 10$; ■, $\tau_0 = 1$. Here ε_0 is the limiting low frequency (or static) permittivity

The parameter $\bar{\beta}$ is related to the breadth of the loss peak and the value of τ_0 is related to the position of the loss peak in the plot $\varepsilon''(\omega)$ *versus* $\log \omega$. For our present calculations we show the experimental loss data as $(G/\omega) = C_0\varepsilon''(\omega)$, where G is electrical conductance, since it is more amenable to practical determination and it obviates the need to know sample thickness and area (to determine C_0). The errors were calculated as the percentage deviation of the results of using the Brather equations from those obtained numerically by Koizumi and Kita[15]. Our calculations were performed for $\tau_0 = 100$, 10 and 1 and for $\bar{\beta} = 0.50$, 0.75 and 1.0 for each τ_0 value. The Hamon approximation values were also calculated for all (β, τ_0) values (since they were a necessary part of the procedure, as step 2).

Figure 1 shows, as an example, the loss curves for fixed $\bar{\beta}$ ($= 0.75$) and different values of τ_0 (100, 10, 1), as obtained using the Brather approximation for $(\varphi(t), t)$ values obeying the KWW function (equation (2)). The loss curves are broad and asymmetric and move to lower frequencies as τ_0 is increased. For $\tau_0 = 1$ only the low-frequency part of the loss peak is obtained, but its determination requires an extrapolation beyond $\log f \approx 0.5$, as described above. This provides a severe test for the application of the Brather approximation. We have determined ε'' (Brather)/ε'' (numerical from ref. 15) for data spanning the frequency range shown in *Figure 1* and for different values of $\bar{\beta}$ and τ_0. *Figures 2a–c* show the percentage error, determined from this ratio, for the particular cases $\tau_0 = 1$ and $\bar{\beta} = 1.0$, 0.75 and 0.50. In all cases the error is less than 4%, except for one point in *Figure 2c*, over the whole frequency range, which is a very satisfactory result. The results for $\bar{\beta} = 1$ are particulary pleasing since it is well known that approximate methods for transforming transient current data into equivalent loss factor data become

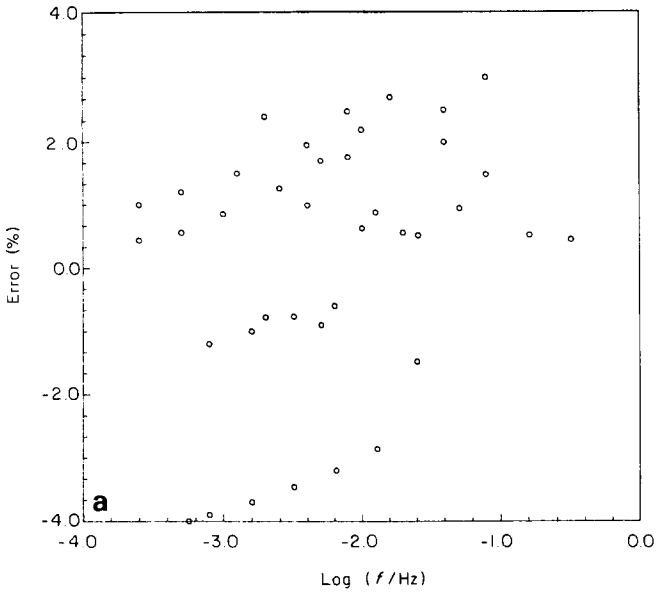

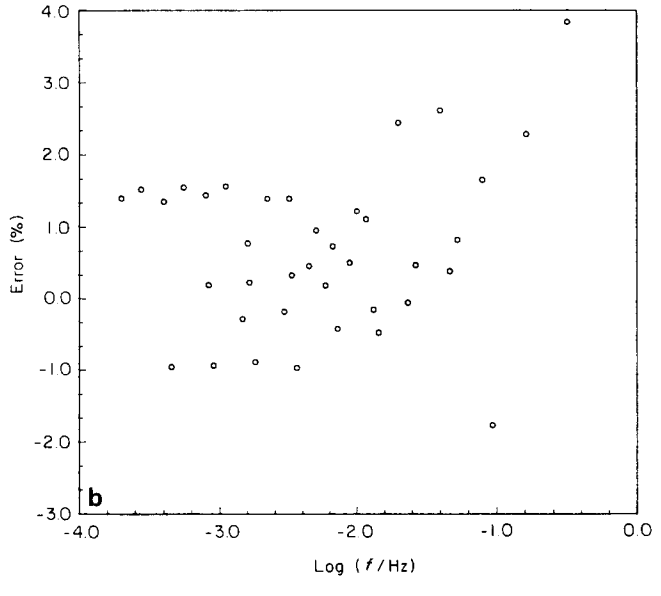

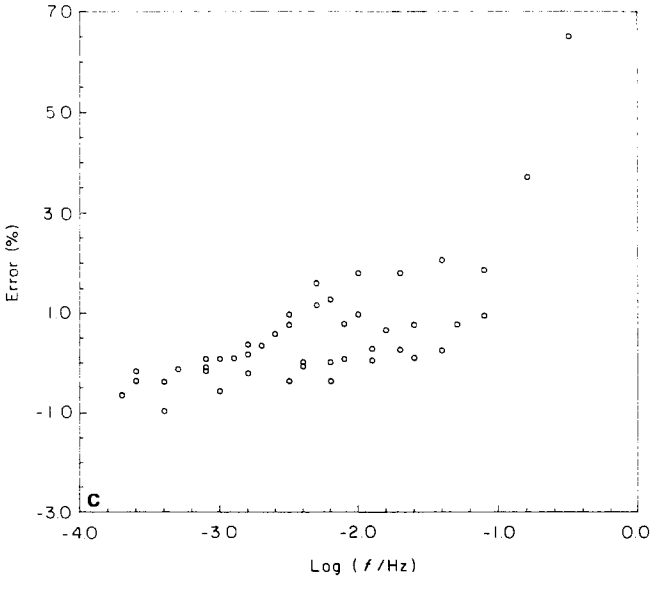

Figure 2 Percentage error for ε'' (Brather) compared with ε'' (calculated) *versus* $\log f$ for $\tau_0 = 1$. (a) $\beta = 1.0$; (b) $\beta = 0.75$; (c) $\beta = 0.50$. Points relate to data of *Figure 1*

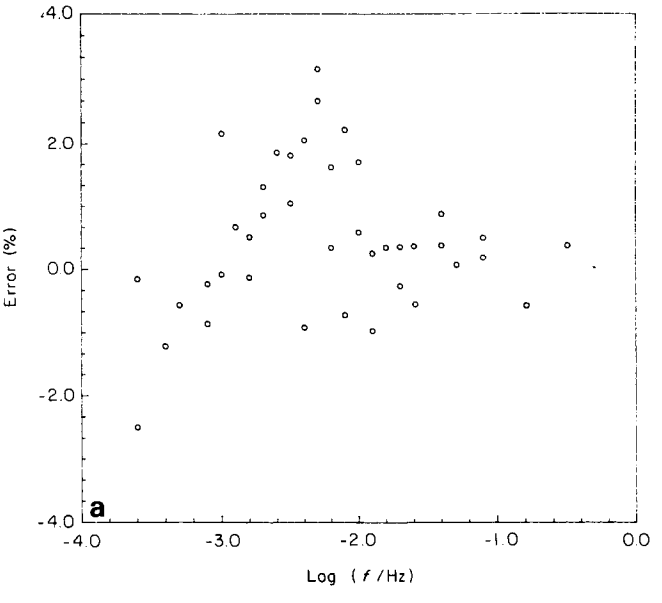

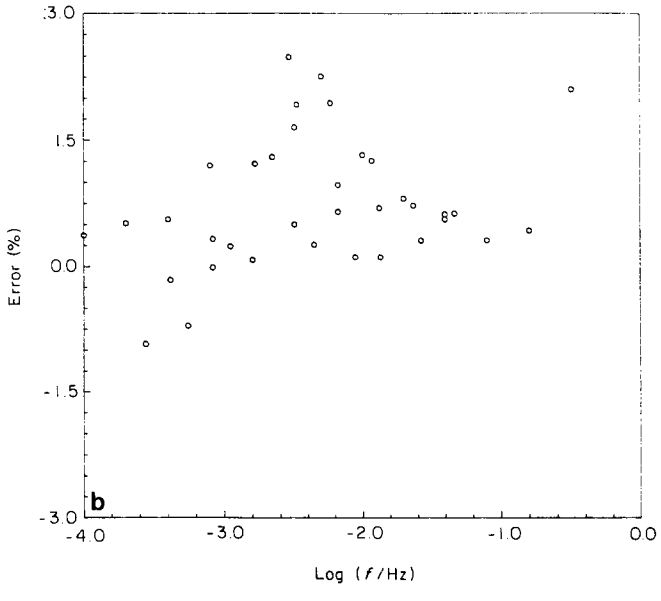

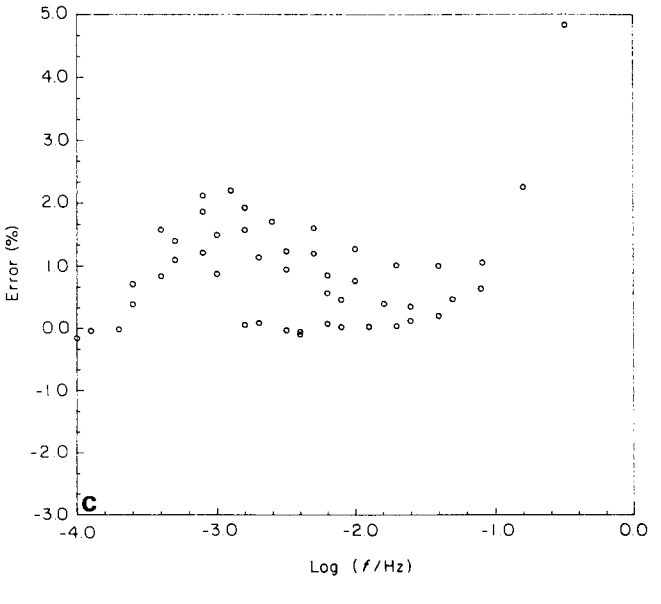

Figure 3 Percentage error for ε'' (Brather) compared with ε'' (calculated) *versus* $\log f$ for $\tau_0 = 10$. (a) $\beta = 1.0$; (b) $\beta = 0.75$; (c) $\beta = 0.50$

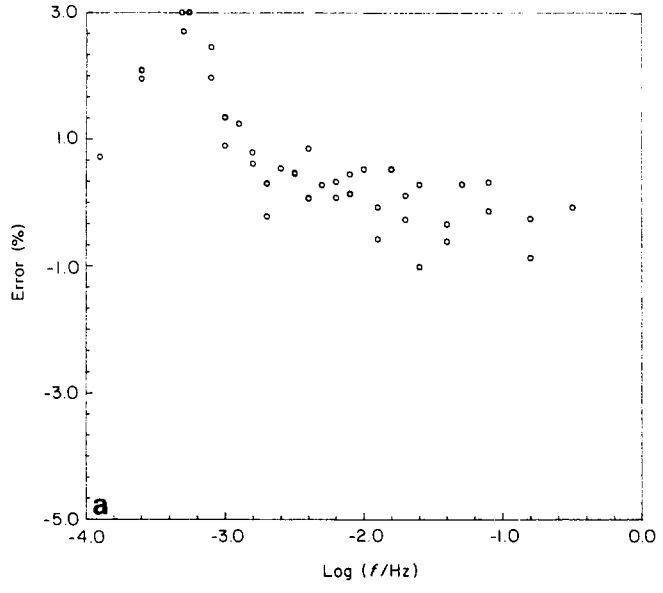

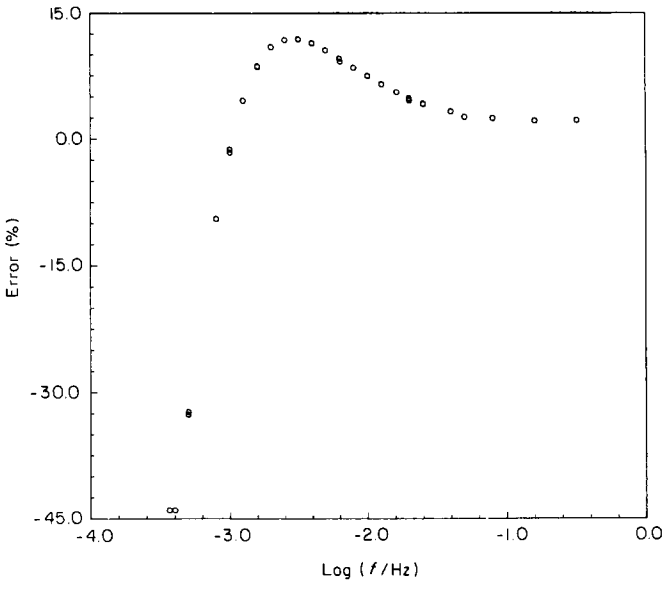

Figure 5 Percentage error for ε'' (Hamon) compared with ε'' (calculated) *versus* $\log f$ for $\tau_0 = 10$, $\bar{\beta} = 0.50$

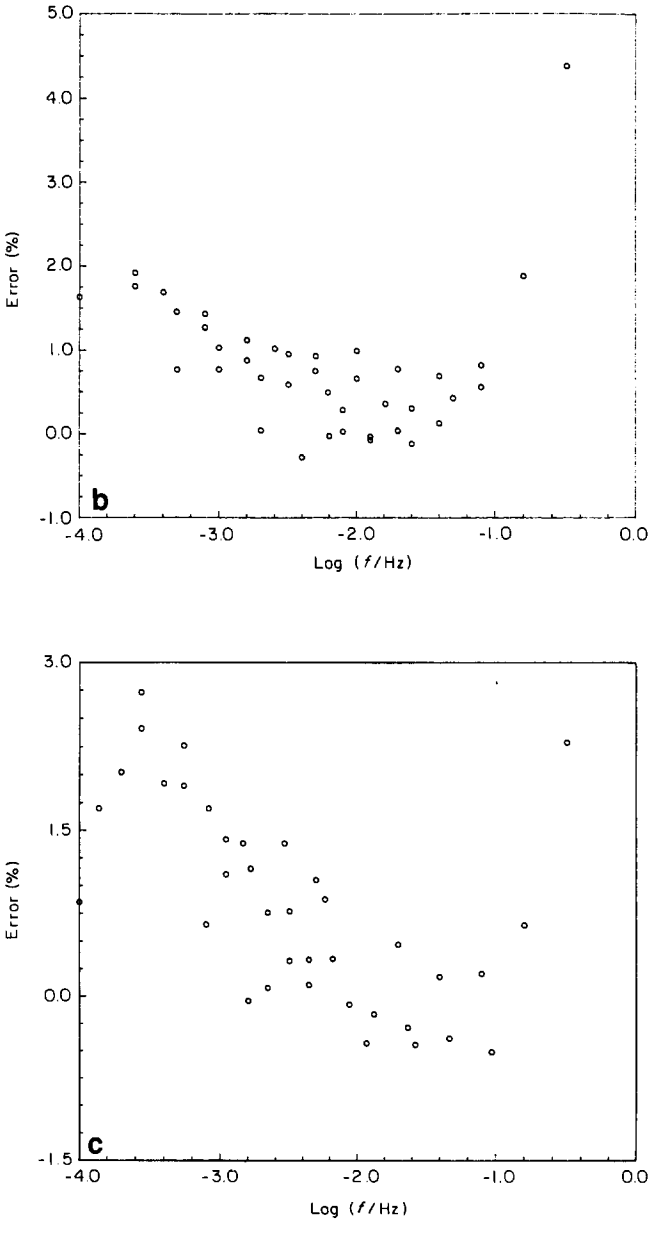

Figure 4 Percentage error for ε'' (Brather) compared with ε'' (calculated) *versus* $\log f$ for $\tau_0 = 100$. (a) $\bar{\beta} = 1.0$; (b) $\bar{\beta} = 0.75$; (c) $\bar{\beta} = 0.50$

less successful as single relaxation-time behaviour is approached[8,11,12,16].

Figures 3a–c and *4a–c* show similar plots to *Figures 2a–c* for the sequences $\tau_0 = 10$, $\bar{\beta} = 1.0, 0.75, 0.50$ and $\tau_0 = 100, \bar{\beta} = 1.0, 0.75, 0.50$. Inspection of *Figure 1* shows that the maximum loss occurs around -2.0 and -3.0 for $\tau_0 = 10$ and $\tau_0 = 100$, respectively, which is true for any value of $\bar{\beta}$. For the sequence shown in *Figures 3a–c* the error curves show a systematic variation with frequency with an error maximum which moves to lower frequencies as $\bar{\beta}$ is decreased. Also, there is an upswing in the error curve which is accentuated as $\bar{\beta}$ is decreased. However, the error values are similar in all cases and the correction could be applied systematically to improve the accuracy of the Brather transformation method if experimental data warranted it. For the sequence in *Figures 4a–c*, again the error curves show a systematic variation with frequancy and an upswing is also noted at higher frequencies; but we also note that this occurs in the high frequency tail of the loss curve (see *Figure 1*). The errors shown in *Figure 4* are small in all cases, and corrections could be applied systematically to transformed experimental transient data if the experimental accuracy warranted it.

The results shown in *Figures 2–4* demonstrate the good accuracy of the Brather approximation when it is applied to the KWW function in a range of $\bar{\beta}$ values commonly observed for polymer relaxations[10–13] and those in glass-forming liquids[14]. The magnitude of these errors contrasts markedly to those of the Hamon approximation[8]. *Figure 5* shows, as an example, the curve for this approximation for the particular case $\tau_0 = 10$, $\bar{\beta} = 0.50$ (for which ε''_{max} occurs at $\log f \approx -2$). For $\log f > 1.5$ the error is less than 5% but at lower frequencies large errors are obtained.

EXPERIMENTAL DATA FOR A LIQUID-CRYSTALLINE POLYMER

To demonstrate the application of the Brather approximation to a polymer system, we have studied a siloxane liquid-crystalline side-chain polymer (LCP 6)

having the following structure:

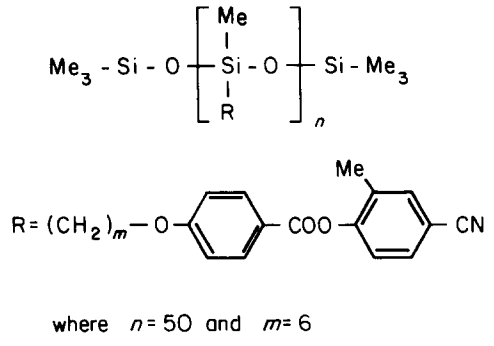

where $n = 50$ and $m = 6$

where $n \approx 50$. This material was kindly provided by Professor G. W. Gray and Dr D. Lacey of Hull University. It has an apparent glass transition temperature (T_g) of 290.3 K and a clearing temperature (T_c) of 325 K. The sample was prepared as a film 1 cm in diameter, 150 μm in thickness and was contained between brass electrodes with poly(tetrafluoroethylene) spaces, to ensure uniformity of thickness, within a three-terminal dielectric cell. The cell temperature was maintained to ± 0.1 K using a controlled water bath. The material was aligned homeotropically by cooling slowly from the melt (cooling rate 0.05 K min^{-1}) into the liquid crystalline state in the presence of 200 V at 800 Hz. The transient discharge current following removal of a charging voltage of 100 V d.c. was measured using a Keithey 617 digital electrometer. The voltage (which was supplied by the electrometer) was maintained for 1 h before the transient decay current was measured. The first data point was at 0.365 s, which sets the lower limit of t_0 in the Brather approximation. Initial currents were $\sim 10^{-11}$ A. The Brather approximation was applied to the data and made use of high-frequency a.c. dielectric data obtained for the sample using a Gen Rad 1689 Digibridge ($10-10^5$ Hz), as described previously[4-6].

Figure 6 shows the results for the homeotropically aligned sample as obtained using the Brather approximation in the range $10^{-0.5}$ to $10^{-3.5}$ Hz. The loss peak is observed and moves rapidly to higher frequencies as

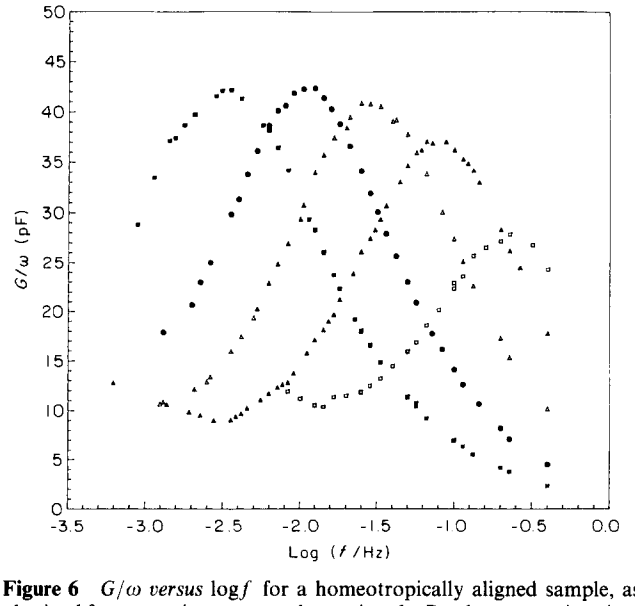

Figure 6 G/ω *versus* log$f$ for a homeotropically aligned sample, as obtained from transient current data using the Brather approximation. ■, 11°C; ●, 14°C; △, 17°C; ▲, 20°C; □, 23°C

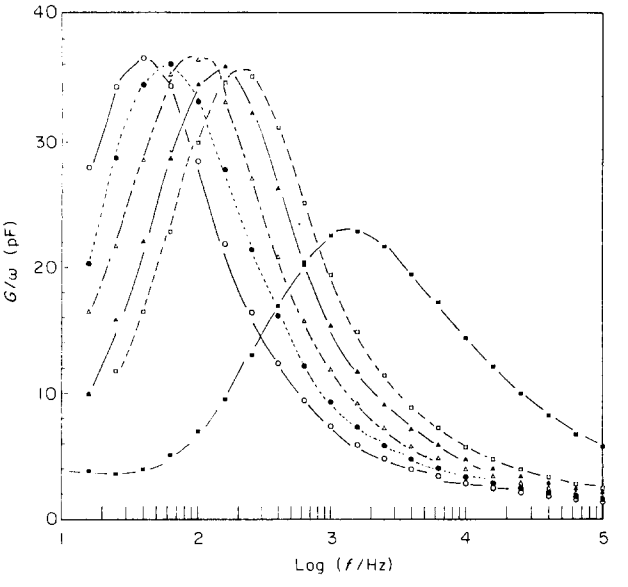

Figure 7 Higher frequency loss curves for the homeotropically aligned sample. ○, 40°C; ●, 42°C; △, 44°C; ▲, 46°C; □, 48°C; ■, sample in isotropic liquid state at 55°C

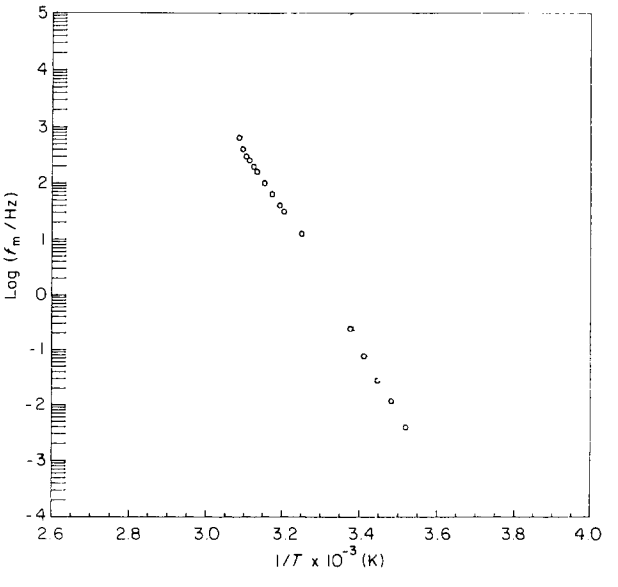

Figure 8 Log f_m *versus* $1/T$ for the homeotropically aligned sample

temperature is increased. For comparison, the loss data for the same sample, obtained in the higher frequency range by the a.c. method, is shown in *Figure 7*, while *Figure 8* shows the plot of $\log f_m$, where f_m is the frequency of maximum loss factor, against reciprocal temperature and covers a frequency range of 5.5 decades. A comparison of *Figures 6* and *7* shows that the loss peaks in the two frequency ranges are of similar height and shape, although the loss peak at 23°C looks far too small. *Figure 8* shows that $\log f_m$ is continuous between the two ranges. We note that the downward curvature of the plot in *Figure 8* is less pronounced than that observed previously[6] for a polymer whose structure is similar to the sample in this work, but having spacers of eight CH_2 units and which forms a smectic rather than a nematic liquid crystalline state. The motions which give rise to the narrow (δ) loss peak for the homeotropic sample correspond to the 00-relaxation mode[5,18] in which the longitudinal component, μ_l of the dipole

moment μ of the mesogenic head group reorientates with respect to the director axis $\tilde{n}$. As the temperature is reduced towards the apparent glass transition temperature T_g, the motions of the head group, which are coupled to the polymer chain motions, slow down markedly, indicating the freezing-in of configurational entropy of the entire sample, the restriction being conferred simultaneously on backbone and side-chain motions. This is one example where knowledge of the wide-frequency behaviour of polymers is necessary to answer questions regarding the relationship between main-chain and side-chain motions[19]. In addition, the use of an ultra-low frequency dielectric technique means overlapping peaks may be better resolved if they have different apparent activation energies. Further, low frequencies are invaluable in examining the ageing properties of polymers since they can probe the motions at low temperatures near T_g where the volume realxation (densification) associated with ageing occurs.

CONCLUSION

The methodology of the Brather approximation, as applied to the determination of ultra-low frequency dielectric loss spectra of polymers, has been described. Its accuracy has been investigated for the particular case of the KWW relaxation function, and is shown to be good if proper care is taken to include high-frequency losses, whether by extrapolation or by independent loss measurements. The Brather approximation has been applied to transient current data obtained for a siloxane liquid crystalline side chain polymer which has been homeotropically aligned; it is shown that the transient data, transformed into the frequency domain complement rather well the high frequency loss data obtained for the same sample.

ACKNOWLEDGEMENTS

We thank Professor G. W. Gray FRS and Dr D. Lacey of Hull University for the provision of the liquid crystalline polymer sample, and the SERC for support under their Electroactive Polymers Initiative.

REFERENCES

1 McCrum, N. G., Read, B. E. and Williams, G. 'Anelastic and Dielectric Effects in Polymeric Solids', Wiley, London, 1967
2 Mopsik, F. I. *Rev. Sci. Instrum.* 1984, **55**, 79
3 Mopsik, F. I. *IEEE Trans. Electr. Insul.* 1985, **EI-20**, 957
4 Attard, G. S., Araki, K., Moura, J. J. and Williams, G. *Liquid Cryst.* 1987, **3**, 861
5 Attard, G. S., Araki, K. and Williams, G. *Br. Polym. J.* 1987, **19**, 119
6 Attard, G. S., Moura-Ramos, J. J. and Williams, G. *J. Polym. Sci., Polym. Phys. Edn* 1987, **25**, 1099
7 Brather, A. *Coll. Polym. Sci.* 1979, **257**, 785
8 Hamon, B. V. *Proc. IEE* 1953, **27**, 99
9 Ribelles, J. L. and Calleja, R. D. *J. Polym. Sci., Polym. Phys. Edn* 1985, **23**, 1505
10 Cook, M., Watts, D. C. and Williams, G. *Trans. Faraday Soc.* 1970, **66**, 2503
11 Williams, G. and Watts, D. C. *Trans Faraday Soc.* 1970, **66**, 80
12 Williams, G., Watts, D. C., Dev, S. B. and North, A. M. *Trans. Faraday Soc.* 1971, **67**, 1323
13 Williams, G., Cook, M. and Hains, P. J. *J. Chem., Soc., Faraday Trans. II* 1972, **68**, 1045
14 Williams, G. in 'Dielectric and Related Molecular Processes' (Ed. M. Davies), Spec. Period Rep., The Chemical Society, London, 1975, Vol. 2, p. 151
15 Koizumi, N. and Kita, Y. *Bull. Inst. Chem. Res. Kyoto Univ.* 1978, **56**, (6), 301
16 Williams, G. *Trans. Faraday Soc.* 1962, **58**, 1041
17 Scheiber, D. J. *J. Res. Natl Bur. Stand.* 1961, **65C**, 23
18 Araki, K., Attard, G. S., Kozak, A., Williams, G., Gray, G. W., Lacey, D. and Nestor, G. *J. Chem. Soc., Faraday Trans. II* 1988, **84**, 1067
19 Plate, N. A., Taltroze, R. V. and Shibaer, V. P. *Makromol. Chem. Makromol Symp.* 1987, **12**, 203